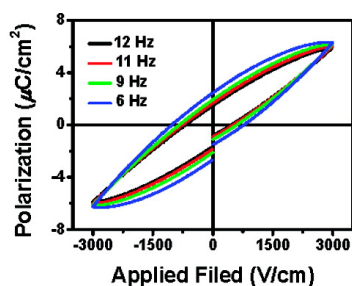
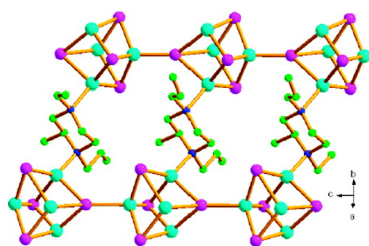


## 3D Framework Containing CuBr Cubane as Connecting Node with Strong Ferroelectricity

Wen Zhang, Ren-Gen Xiong, and Songping D. Huang

*J. Am. Chem. Soc.*, **2008**, 130 (32), 10468-10469 • DOI: 10.1021/ja803021v • Publication Date (Web): 18 July 2008

Downloaded from <http://pubs.acs.org> on February 8, 2009



### More About This Article

Additional resources and features associated with this article are available within the HTML version:

- Supporting Information
- Links to the 1 articles that cite this article, as of the time of this article download
- Access to high resolution figures
- Links to articles and content related to this article
- Copyright permission to reproduce figures and/or text from this article

[View the Full Text HTML](#)

## 3D Framework Containing $\text{Cu}_4\text{Br}_4$ Cubane as Connecting Node with Strong Ferroelectricity

Wen Zhang,<sup>†</sup> Ren-Gen Xiong,<sup>\*,†</sup> and Songping D. Huang<sup>\*,†</sup>

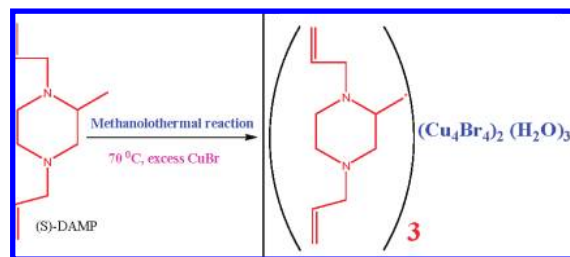
Ordered Matter Science Research Center, Southeast University, Nanjing 211189, P. R. China, and  
Chemistry Department, Kent State University, Kent, Ohio 44240

Received April 24, 2008; E-mail: xiongrg@seu.edu.cn; shuang1@kent.edu

The movement and storage of electrical charges and the manipulation of the electric fields they produce are the basis of the operation of computer processors and memories. The modern electronics industry demands an ever greater decrease in switching time and length scales, approaching the level of individual electrons and atoms. Although continued improvements in conventional semiconductor designs can to some extent address these needs, there is increasing motivation to consider alternative paradigms. In ferroelectric oxides,<sup>1,2</sup> electric polarization, bond charges, and large electric fields are produced by displacements of individual atoms, and devices based on ferroelectric materials therefore can be made in principle to operate on atomic scale. However, current ferroelectrics is only limited to metal–titanate whose synthesis demands strict reaction conditions such as high temperature (500 °C), etc. A molecule-based MOF (metal–organic framework)-containing cluster as a connecting node may mimic the behavior of its ferroelectricity because its synthesis is at a relatively low temperature (<200 °C) and easily accessible. As continuation of our systematic investigations on ferroelectric MOFs,<sup>3–9</sup> we have realized that  $\text{CuX}$  ( $X = \text{halogen}$ ) can easily form a cluster to mimic the pure inorganic part. Herein we used a homochiral ligand containing two bridging N atoms as connecting points to react with excess  $\text{CuBr}$  to obtain a MOF **1** in which the 3D framework contains a cubane-like cluster used as four connecting nodes to extend this structure. The methanolothermal reaction of (*S*)-1,4-diallyl-2-methylpiperazine (DAMP) with an excess  $\text{CuBr}$  affords a novel homochiral 3D framework  $(\text{DAMP})_3(\text{Cu}_4\text{Br}_4)_2(\text{H}_2\text{O})_3$  (**1**), as shown in Scheme 1 (see Supporting Information).

The X-ray crystal structural determination reveals that each local coordination environment around the Cu center can be best described as a slightly distorted tetrahedron in which three  $\mu_3$ -Br atoms and one N atom from an (*S*)-DAMP ligand compose four coordination bonds around the Cu1 center while three  $\mu_3$ -Br atoms and one  $\mu_4$ -Br atom compose a four-bonding geometry around the Cu2 center as shown in Figure 1 (see Supporting Information). Thus, there are two kinds of bridging Br atoms ( $\mu_3$ -Br atoms and one  $\mu_4$ -Br atom), while a  $\mu_4$ -Br atom connects two cubanes ( $\text{Cu}_4\text{Br}_4$ ) to result in the formation of a 1D chain where the cubane is the smallest repeating unit as depicted in Figure 2. Interestingly, the organic ligand DAMP and the  $\mu_4$ -Br atoms connect the Cu atoms in three directions to result in the formation of a 3D framework as shown in Figure 2. To make this topology simple, DAMP can be considered as a long line so that the 3D framework can be considered as  $6^6$  net where each hexagonal connecting node is composed of one cubane  $\text{Cu}_4\text{Br}_4$  as shown in Figure 3. Water molecules forming pale yellow tanks are included in the hexagonal channel (as shown in Figure 2 and Figure 3). The framework may

Scheme 1



be stable between the temperature of 158 and 300 °C. (see Supporting Information).

Given that the product MOF **1** crystallizes in a chiral space group ( $P3$ ) while it also adopts a polar point group  $C_3$  belonging to one of 10 polar point groups ( $C_1, C_2, C_3, C_{2v}, C_4, C_{4v}, C_3, C_{3v}, C_6, C_{6v}$ ) where the ferroelectric and second harmonic generation will occur, its optical properties were investigated. Preliminary studies of a powdered sample indicate that MOF **1** is more SHG active ca. 2~10 times than that of KDP. Experimental results indicate that MOF **1** does indeed display ferroelectric behavior. Figure 4 clearly shows an electric hysteresis loop occurred, which is a typical ferroelectric feature, with a remanent polarization ( $P_r$ ) of ca.  $1.4\sim 2.5 \mu\text{C}\cdot\text{cm}^{-2}$  (sample electrode area/needle area is about 100 times so that real  $P_r$  value should be 140/100 and 250/100) and a coercive field ( $E_c$ ) of ca.  $0.65\sim 1.0 \text{KV}\cdot\text{cm}^{-1}$ . The saturation spontaneous polarization ( $P_s$ ) of MOF **1** is ca.  $6.3 \mu\text{C}/\text{cm}^2$  which is much larger than those found in a multiferroic MOF  $\text{Rb}^{1}_{0.82}\text{Mn}^{\text{II}}_{0.20}\text{Mn}^{\text{III}}_{0.80}\text{[Fe}^{\text{II}}(\text{CN})_6]_{0.80}\text{[Fe}^{\text{III}}(\text{CN})_6]_{0.14}\cdot\text{H}_2\text{O}$  ( $P_s \approx 0.21 \mu\text{C}/\text{cm}^2$ ),<sup>9a</sup> a MOF with tetrazole  $\text{Cd}(\text{TBP})(\text{Cl})$  ( $\text{TBP} = N$ -(4'-tetrazoyl-benzyl)proline)

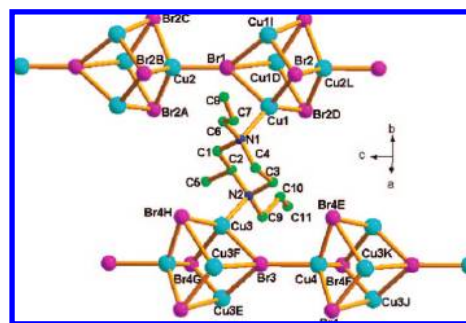
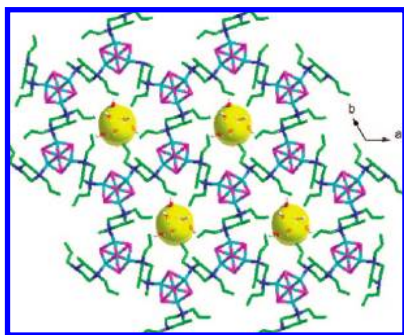


Figure 1. An asymmetric unit representation of MOF **1** showing that there are two types of Cu atoms with different coordination environments (coordinated with four Br atoms or with three Br atoms and one N atom from DAMP) and two kinds of bridging Br ( $\mu_4$  and  $\mu_3$ ), and the homochiral organic ligands act as bidentate linkers to connect the two cubane  $\text{Cu}_4\text{Br}_4$  units. Typical bond distances (Å) are given as follows: Cu1–N1, 2.132(8); Cu3–N2, 2.031 (9); Cu1–Br1, 2.6467(19); Cu1–Br2, 2.5125 (17); Cu2–Br1, 2.427(3); Cu3–Br3, 2.5818(19); Cu4–Br3, 2.552(3); Cu4–Br4, 2.4538 (13).

<sup>†</sup> Southeast University.

<sup>‡</sup> Kent State University.



**Figure 2.** 3D representation of MOF 1 showing that three water molecules are included in the hexagonal channel.

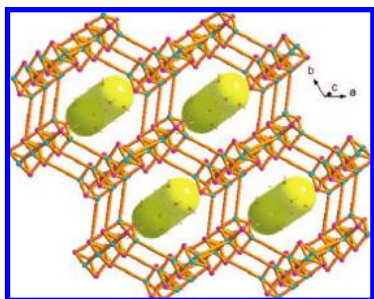


**Figure 3.** Simplified 3D representation of MOF 1 where DAMP is abbreviated as a long line in which each hexagon is composed of six-cubane  $\text{Cu}_4\text{Br}_4$  units as connecting nodes where water molecules are included in hexagonal channel.

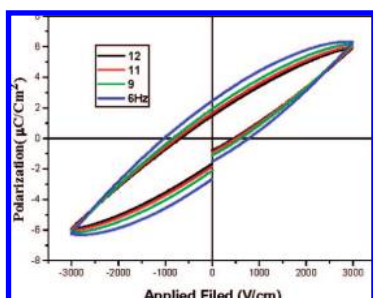


**Figure 4.** Polarization versus applied electric field at different frequencies for MOF 1.

( $P_s \approx 0.50 \mu\text{C}/\text{cm}^2$ )<sup>9b</sup> and molecule-based lanthanide compound  $[\text{Eu}(\text{tta})_3](\text{L})$  ( $\text{tta} = 2$ -thenoyltrifluoroacetato,  $\text{L} = (R,R)$ -(-)-4,5-pinene bipyridine) ( $P_s \approx 0.1 \mu\text{C}/\text{cm}^2$ )<sup>9c</sup> as well as  $\text{Ni}_3\text{O}(\text{ClO}_4)_4(\text{TBPLA})_2$  ( $\text{TBPLA} = (S)$ -1,1'1''-(2,4,6-trimethylbenzene-1,3,5-triyl)tris(methylene)]tris(pyrrolidine-2-carboxylic acid) ( $P_s \approx 3.4 \text{ nC}/\text{cm}^2$ )<sup>9d</sup>. In comparison, the  $P_s$  of MOF 1 is still larger than that of KDP ( $P_s \approx 5.0 \mu\text{C}/\text{cm}^2$ )<sup>9e</sup> and comparable to the  $P_s$  with a value of  $6.5 \mu\text{C}/\text{cm}^2$  that was reported for a typical ferroelectric  $\text{BaTiO}_3$  synthesized by the peptide-assisted synthesis method where its  $P_r$  value is  $\sim 2.5$ .<sup>10</sup> From Figure 4 it can be found that the  $P_r$  increases gradually as frequency decreases, indicating that its ferroelectricity is a lower frequency-dependent material. Also, it is found in Figure 5 that the  $P_r$  value gradually changes a little bit with applied electric field. It is worth noting that a highly applied electric field forces MOF 1 to display large dielectric loss (or electric leakage). More importantly, a low applied electric field can polarize this sample to be ferroelectrics, meaning practical

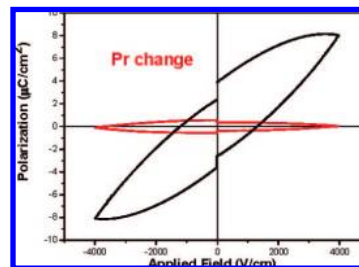


**Figure 5.**  $P_r$  changes of MOF 1 with applied electric field in which  $P_r$  almost remains unchanged (for more information, see Supporting Information).

utilization, compared to that  $\text{BaTiO}_3$  obtained by peptide-assisted synthesis where its  $E_c$  is about  $7\sim 8 \text{ KV}/\text{cm}$ , much larger than that of current MOF 1. To the best of our knowledge, MOF 1 represents the first example of inorganic-organic hybrid compounds that exhibit such large ferroelectric  $P_r$  and  $P_s$  values, probably due to the  $\text{Cu}_4\text{Br}_4$  cubane anion having a large polarizability<sup>11</sup> (for more, see Supporting Information).

In conclusion, we have successfully utilized  $\text{CuBr}$  as a cluster connecting node to mimic the pure inorganic role in ferroelectrics to enhance its  $P_s$  value. This will open up a new avenue through a crystal engineering strategy for the construction of a polar MOF with ferroelectric properties.

**Acknowledgment.** This work was supported by Project 973, the National Natural Science Foundation of China (20490214, 50673039, and 20540420518), and the Cultivation Fund of the Key Scientific and Technical Innovation Project, MOE of China (2005).

**Supporting Information Available:** X-ray crystallographic cif file, TGA,  $P$ - $E$  curve for dehydrated MOF 1 at 12 Hz, XRD powder patterns, and other framework representations. This material is available free of charge via the Internet at <http://pubs.acs.org>.

## References

- (1) Rijnders, G.; Blank, D. H. A. *Nature* **2005**, *433*, 369.
- (2) Lee, H. N.; Christen, H. M.; Chisholm, M. F.; Rouleau, C. M.; Lowndes, D. H. *Nature* **2005**, *433*, 395.
- (3) Fu, D.-W.; Ye, H.-Y.; Ye, Q.; Pan, K.-J.; Xiong, R.-G. *J. Chem. Soc., Dalton Trans.* **2008**, 874.
- (4) Zhao, H.; Ye, Q.; Qu, Z.-R.; Fu, D. W.; Xiong, R.-G.; Huang, S.-P. D.; Chan, P. W. H. *Chem.-Eur. J.* **2008**, *14*, 1164.
- (5) Ye, Q.; Fu, D.-W.; Tian, H.; Xiong, R.-G.; Chan, P. W. H.; Huang, S.-P. D. *Inorg. Chem.* **2008**, *47*, 772.
- (6) Zhao, H.; Qu, Z.-R.; Ye, H.-Y.; Xiong, R.-G. *Chem. Soc. Rev.* **2008**, *37*, 84.
- (7) Ye, Q.; Song, Y.-M.; Fu, D.-W.; Wang, G.-X.; Xiong, R.-G.; Chan, P. W. H.; Huang, S.-P. D. *Cryst. Growth Des.* **2007**, *7*, 1568.
- (8) Gu, Z.-G.; Zhou, X.-H.; Jin, Y.-B.; Xiong, R.-G.; Zuo, J.-L.; You, X.-Z. *Inorg. Chem.* **2007**, *46*, 5462.
- (9) (a) Ohkoshi, S.; Tokoro, H.; Matsuda, T.; Takahashi, H.; Irie, H.; Hashimoto, K. *Angew. Chem., Int. Ed.* **2007**, *46*, 3238. (b) Ye, Q.; Song, Y.-M.; Wang, G.-X.; Fu, D.-W.; Chen, K.; Chan, P. W. H.; Zhu, J.-S.; Huang, D. S.; Xiong, R.-G. *J. Am. Chem. Soc.* **2006**, *128*, 6554. (c) Li, X.-L.; Chen, K.; Liu, Y.; Wang, Z.-X.; Wang, T.-W.; Zuo, J.-L.; Li, Y.-Z.; Wang, Y.; Zhu, J.-S.; Liu, J.-M.; Song, Y.; You, X.-Z. *Angew. Chem., Int. Ed.* **2007**, *46*, 6820. (d) Fu, D.-W.; Song, Y.-M.; Wang, G.-X.; Ye, Q.; Xiong, R.-G.; Akutagawa, T.; Nakamura, T.; Chan, P. W. H.; Huang, D. S. *J. Am. Chem. Soc.* **2007**, *129*, 5346. (e) Zhao, H.; Qu, Z.-R.; Ye, Q.; Abrahams, B. F.; Wang, Y.-P.; Liu, Z.-G.; Xue, Z.-L.; Xiong, R.-G.; You, X.-Z. *Chem. Mater.* **2003**, *15*, 4166.
- (10) Ahmad, G.; Dickerson, M. B.; Cai, Y.; Jones, S. E.; Ernst, E. M.; Vernon, J. P.; Haluska, M. S.; Fang, Y.; Wang, J.; Subramanyam, G.; Naik, R. R.; Sandhage, K. H. *J. Am. Chem. Soc.* **2008**, *130*, 4.
- (11) (a) Ye, Q.; Zhao, H.; Qu, Z.-R.; Fu, D.-W.; Xiong, R.-G.; Cui, Y.-P.; Akutagawa, T.; Chan, P. W. H.; Nakamura, T. *Angew. Chem., Int. Ed.* **2007**, *46*, 6852. (b) Wang, G.-X.; Xiong, R.-G. *Chin. J. Chem.* **2007**, *25*, 1405.

JA803021V